599.
12. Dewitte, W. J.; Liu, L.; Mei, E.; Dye, J. L.; Popov, A. I. *J. Solution Chem.* **1977**, *6*, 337.
13. Buschmann, H.-J. *Inorganic Chim. Acta* **1992**, *195*, 51.
14. (a) Inoue, Y.; Liu, Y.; Hakushi, T. in *Cation Binding by Macrocycles;* Inoue, Y.; Gokel, G. W., Ed.; Marcel Dekker: New York, U. S. A., 1990; Chapter 1. (b) Takeda, Y. in *Cation Binding by Macrocycles*; Inoue, Y.; Gokel, G. W. Ed.; Marcel Dekker: New York, U. S. A., 1990; Chapter 3.
15. Ono, K.; Konami, H.; Murakami, K. *Polym. Prepr., Am. Chem. Soc., Div. Polym. Chem.* **1979**, *20*, 1015.
16. Lee, S. S.; Kim, D. Y.; Jung, J. H.; Kim, S.-J. *71st Annual Meeting of the Korean Chemical Society, Seoul, Korea,* **1993**, Abstract, 146.
17. Wakita, R.; Miyakoshi, M.; Nakatsuguji, Y.; Okahara, M. *J. Incl. Phenom.* **1991**, *10*, 127.
18. Jung, J. H.; Lee, S. S.; *Bull. Kor. Chem. Soc.* in preparation.
19. Gordon A. J.; Ford, R. A. in *The Chemist's Companion*; Wiley: U. S. A., 1972; p. 433.
20. Takeda, Y.; Yano, H.; Ishibashi, M.; Isozumi, H. *Bull. Chem. Soc. Jpn.* **1980**, *53*, 72.
21. Gates, S. C.; Becker, J. in *Laboratory Automization Using the IBM PC*; Prentice-Hall: Englewood Cliffs, U. S. A., 1989.
22. Dye, J. L.; Nicely, V. A. *J. Chem. Edu.* **1971**, *48*, 443.
23. Hopkins, Jr., H. P.; Norman, A. B. *J. Phys. Chem.* **1980**, *84*, 309.
24. Lee, S. S.; Park, S. O.; Jung, J. H.; Lee, B. Y. *Bull. Kor. Chem. Soc.* **1990**, *11*, 276.
25. Pearson, R. G.; *J. Am. Chem. Soc.* **1963**, *85*, 3663.
26. Zhu, C. Y.; Izatt, R. M.; Bradshaw, J. S.; Dalley, N. K. *J. Incl. Phenom.* **1992**, *13*, 17.
27. Lindoy, S. F.; Lip, H. C.; Rea, J. H.; Smith, R. H.; Tasker, P. A. *Inorg. Chem.* **1980**, *19*, 3360.
28. Sieger, H.; Vögtle, H. *Angew. Chem. Int. Ed. Engl.* **1978**, *17*, 198.

Characteristics of Products in the Reaction 40 MeV/nucleon $^{14}N+Ag$

Yong Hee Chung* and N. T. Porile

**Department of Chemistry, Hallym University, Chuncheon 200-702*
Department of Chemistry, Purdue University, W. Lafayette, Indiana 47907, USA
Received August 2, 1994

Cross sections and recoil properties have been measured for the fragments produced in the interaction of silver with 40 MeV/nucleon ^{14}N ions using off-line γ-ray spectroscopy. The data were used to obtain the isobaric-yield distribution, the mass yield distribution, and the fractional momentum transfer. The values of forward-to-backward ratios were measured to be very large, indicating that substantial momentum transfer occurs at this energy regime. The results are compared with other studies of the interaction of silver with intermediate-energy heavy ions.

Introduction

Nuclear reactions in intermediate-energy regime have attracted considerable interest in recent years because of the change in the reaction dynamics. In low-energy regime(<10 MeV/nucleon) nuclear reactions are dominated by mean-field dynamics, characterized by complete fusion. On the other hand, nuclear reactions in high-energy regime(>100 MeV/nucleon) involve the dynamics of nucleon-nucleon interactions, signified by fragmentation. The intermediate-energy reactions must therefore experience the onset of high-energy reaction processes.

Several intermediate-energy heavy ion reactions have been studied. Lund *et al.*[1-3] found that the high-energy dynamics are operative in the interaction of silver with 86 MeV/nucleon ^{12}C ions. Multiple dissociation of heavy ion projectiles has been observed at 32.5 MeV/nucleon.[4] In the O-induced reactions on Al, Ni, and Au targets, breakup of the projectile was reported by Badalà *et al.*[5]

In this work, the results for the study on the interaction of silver with 40 MeV/nucleon ^{14}N ions are presented. The cross sections and recoil properties of the reaction products were obtained utilizing recoil-ranges techniques, as mentioned in our previous works.[6-8] The isobaric-yield distribution, the mass yield distribution, and the fractional momentum transfer are deduced from the data.

Experimental

The experiment was performed at the K500 cyclotron of the National Superconducting Cyclotron Laboratory(NSCL) at Michigan State University. The target stack consisted of silver foil, 30.0 mg/cm^2 thick, surrounded by 10.1 mg/cm^2 thick Mylar foils. The stack was surrounded by two additional Mylar foils, which served to guard the other foils from possible external sources of radioactive products.

The target stack was mounted on an aluminum foil holder, located in an evacuated chamber and irradiated with 40

Table 1. Cross Sections for the Production of Radionuclides in the Interaction of Silver with 40 MeV/nucleon ^{14}N Ions

Nuclide	Type	σ(mb)	Nuclide	Type	σ(mb)
$^{24}Na^{a)}$	C^-	1.93± 0.20	$^{95}Tc^m$	PC^+	3.30± 0.18
$^{28}Mg^{a)}$	C^-	0.49± 0.05	^{95}Ru	C^+	40.1± 2.1
$^{44}Sc^m$	I	0.32± 0.02	^{96}Nb	I	4.24± 0.60
^{46}Sc	I	0.90± 0.05	^{96}Tc	I	23.7± 1.2
^{48}Sc	I	0.08± 0.02	^{97}Ru	C^+	108± 11
^{48}V	C^+	0.46± 0.02	^{97}Rh	PC^+	30.0± 2.0
^{59}Fe	C^-	0.16± 0.02	^{99}Rh	PC^+	6.86± 0.37
^{65}Zn	C^+	2.55± 0.27	$^{99}Rh^m$	PC^+	77.0± 4.0
^{69}Ge	C^+	2.63± 0.16	^{99}Pd	C^+	19.1± 1.1
^{74}As	I	1.40± 0.08	^{100}Rh	I	21.8± 1.9
^{76}Kr	C^+	1.69± 0.15	^{100}Pd	C^+	46.3± 2.4
^{77}Br	C^+	8.38± 0.86	^{101}Rh	PC^+	0.12± 0.01
^{79}Kr	C^+	11.2± 0.7	$^{101}Rh^m$	PC^+	113± 6
^{81}Rb	PC^+	20.6± 2.1	^{101}Pd	C^+	61.1± 3.4
^{83}Rb	C^+	43.6± 2.3	^{102}Rh	I	0.011± 0.001
^{86}Y	I	25.4± 1.3	^{102}Ag	PC^+	31.3± 2.3
^{86}Zr	C^+	18.9± 1.9	^{103}Ru	C^-	1.41± 0.29
^{87}Y	PC^+	75.6± 3.9	^{103}Ag	C^+	42.4± 2.2
^{89}Zr	C^+	91.0± 9.1	^{104}Ag	PC^+	61.1± 3.3
^{89}Nb	PC^+	61.6± 17.0	^{105}Ag	PC^+	126± 6
$^{90}Y^m$	I	0.32± 0.04	^{105}Cd	C^+	21.9± 2.2
^{90}Nb	C^+	47.0± 3.1	$^{106}Rh^m$	I	1.46± 0.17
^{90}Mo	C^+	22.4± 1.1	$^{106}Ag^m$	I	36.9± 1.9
$^{93}Mo^m$	I	24.5± 1.3	^{107}In	C^+	25.4± 3.4
^{93}Tc	PC^+	60.8± 3.3	$^{108}In^m$	I	4.29± 0.30
^{94}Tc	I	40.6± 2.2	^{109}In	C^+	4.77± 0.27
^{94}Ru	C^+	17.4± 0.9	^{112}Pd	C^-	13.7± 3.3
^{95}Nb	C^-	0.83± 0.09	^{112}Ag	C^-	3.76± 0.77
^{95}Tc	PC^+	45.4± 7.9			

[a] The cross sections include those produced from the interaction of Mylar foils with ^{14}N ions.

MeV/nucleon ^{14}N ions. The mean energy at the center of the target was reduced to 38.6 MeV/nucleon, owing to energy degradation in Mylar foils and silver targets.[9] Two irradiations were performed with a duration of 30 min and 3 h. Charge collected in a Faraday cup was recorded with a current integrator. The beam intensity was 15 enA.

Following bombardment, the foils were assayed with calibrated Ge(Li) or intrinsic Ge γ-ray spectrometers. The foils from the short irradiation were assayed at NSCL for about 1 d, while those from the longer irradiation at Purdue for several months. The spectra were analyzed with the code SAMPO,[10] and decay curves were analyzed with the CLSQ code.[11] Nuclidic assignments were based on γ-ray energy and half-life, and confirmed by examining the relative intensities of all measured γ-rays emitted by a presumed nuclide.[12]

Results and Discussion

Cross sections were determined for 57 nuclides, and listed in Table 1. Each of the listed values is the weighted average of results for several γ-rays from two irradiations. The tabulated uncertainties contain the errors derived from the SAMPO and CLSQ fits and also include a 5% error in detector efficiencies. Since Mylar is a brand name for polyethylene terephthalate[$(C_{10}H_4O_2)_n$], ^{24}Na can be produced in the interactions of carbon and oxygen atoms with ^{14}N ions and ^{28}Mg only in the interaction of oxygen with ^{14}N ions. Consequently, the cross sections for ^{24}Na and ^{28}Mg include those produced by the interaction of Mylar foils with ^{14}N ions. In our previous study of the interaction of silver with 15-45 MeV/nucleon ^{12}C ions,[6] the cross sections for ^{24}Na were reduced by 4-7% using the results from the interaction of Mylar with ^{12}C ions, even though ^{28}Mg had not been observed. However, the correction for the cross sections of ^{24}Na and ^{28}Mg in this work might be much larger than those derived from the interaction of Mylar with ^{12}C. While some of the cross sections represent independent yields, denoted as I in Table 1, the majority are cumulative. These are denoted by either C^+ or C^-, depending on whether they include the yields of more neutron-deficient or neutron-excessive isobaric precursors, respectively. In some cases, the measured cross sections include only a partial contribution from isobaric precursors, which is denoted by either PC^+ or PC^-. In the interaction of silver with 25.2 GeV ^{12}C ions and 300 GeV protons,[13] nuclides with mass number higher than the target mass have not been observed. However, products with mass number higher than the target mass have been measured in this work, implying that fusion mechanism could play a role at this energy.

Table 2. Parameters Obtained from the Fit of Eq.(1) to the Cross Sections of Products from the Interaction of Silver with 40 MeV/nucleon ^{14}N Ions

Parameter	Value
α_1	37.9± 1.0
α_2	−1.82± 0.04
α_3	(2.72± 0.05)×10^{-2}
α_4	−(1.24± 0.02)×10^{-4}
α_5	0.525± 0.489
α_6	−(4.96± 1.15)×10^{-2}
α_7	(3.99± 0.65)×10^{-4}
α_8	2.09± 0.07
α_9	0.469± 0.001
α_{10}	−(1.62± 0.12)×10^{-4}

The cross sections measured in this work represent only a fraction of the total mass yield. In order to obtain the mass yield distribution, it is necessary to estimate the unmeasured cross sections. As discussed in our previous work,[6-8] we used a modified form of the Rudstam equation[14] to estimate the unmeasured cross sections. The best fit to the measured cross sections was obtained using the following 10-parameter equation:

$$\sigma(Z,A)=\exp[\alpha_1+\alpha_2 A+\alpha_3 A^2+\alpha_4 A^3 + (\alpha_5+\alpha_6 A+\alpha_7 A^2)|Z_p-Z|^{\alpha_8}] \quad (1)$$

The first four parameters $\alpha_1-\alpha_4$ determine the shape of the mass yield distribution, while the parameters $\alpha_5-\alpha_7$ determine the width of the isobaric-yield distribution. The two A-dependent terms are included to allow for a possible mass dependence in the width. The parameter α_8 determines the shape of the isobaric-yield distribution at a given mass num-

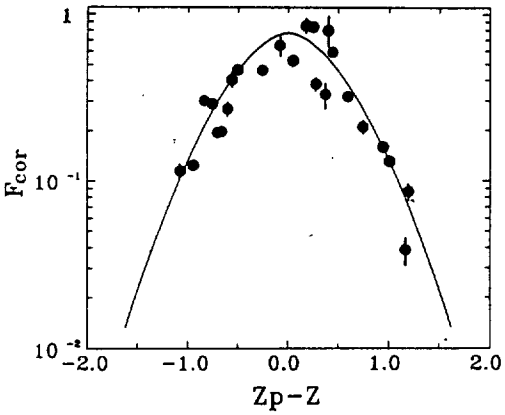

Figure 1. Fractional isobaric-yield distribution for the interaction of silver with 40 MeV/nucleon ^{14}N ions. Curve, fitted values at A=70; points, data scaled to A=70.

ber, where $\alpha_8=2$ corresponds to a Gaussian distribution. The isobaric-yield distribution is assumed to be symmetric about the most probable charge Z_p, which is parametrized as

$$Z_p=\alpha_9 A+\alpha_{10}A^2 \quad (2)$$

The measured cross sections in the $A=44-109$ mass range were fitted with Eq.(1) by means of a nonlinear iterative least-squares code. In the first iteration, Eq.(1) was fitted to both cumulative and independent yields. The cumulative cross sections were then corrected for isobaric feed-in by means of the calculated progenitor cross sections, and the remaining independent yields were refitted. This procedure converged after five iterations. Table 2 lists the values of the parameters $\alpha_1-\alpha_{10}$.

A comparison of the data with the calculated isobaric-yield distribution is shown in Figure 1. The independent yields deduced from the measured cross sections are compared with the isobaric-yield distribution by means of fractional isobaric yields, F. The fractional isobaric yields are obtained by dividing both experimental and calculated cross sections by the calculated total isobaric cross section. The experimental values of F are scaled to a common mass number, A=70, using the ratio of calculated F values at A=70 and at the mass number in question. As shown in Figure 1, the scaled fractional yields are designated Fcor and the parametrization provides a fair fit to the isobaric-yield distribution.

Figure 2 shows a comparison of the measured cumulative cross sections, corrected for the missing yield at each mass number, with the fitted mass yield distribution. The uncertainties in the corrected data points include 30% uncertainties in the values of the unmeasured isotopic cross sections. Eq.(1) and (2) provide a satisfactory representation of the mass yield distribution. The mass yield distribution goes through a minimum at A~50-60 and a maximum at A~90-100. A similar minimum in the mass yield distribution was observed in the interactions of silver with 45 MeV/nucleon and 2.1 GeV/nucleon ^{12}C ions.[6,13] Even though the projectile mass is larger by 2 in mass number than those at the higher energies, a shape of the mass yield distribution has not been altered. The total reaction cross section, R, can be obtained by integrating the mass yield distribution. The value obtained by integration between A=52 and A=119 is 2.87± 0.43

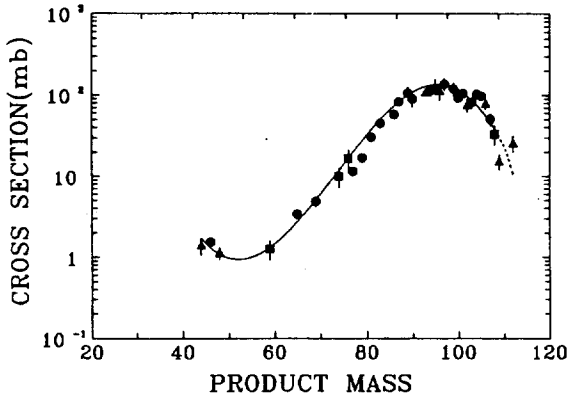

Figure 2. Mass yield distribution for the interaction of silver with 40 MeV/nucleon ^{14}N ions. Solid curve, fit to data. Dashed curve, extrapolation. Points, experimental cross sections corrected for unmeasured yields. The different symbols indicate the fraction of each yield that was measured: ●, >50%; ▲, 20~50%; ■, <20%.

Table 3. Recoil Properties of Products from the Interaction of Silver with 40 MeV/nucleon ^{14}N Ions

Nuclide	2W(F+B)(mg/cm^2)	F/B
$^{44}Sc^m$	9.90± 0.59	6.87± 0.56
^{46}Sc	6.61± 0.33	
^{48}Sc	9.71± 3.72	
^{48}V	6.63± 0.26	
^{59}Fe	7.95± 3.01	
^{65}Zn	5.36± 0.40	
^{69}Ge	3.06± 0.43	
^{74}As	3.87± 0.18	
^{76}Kr	6.11± 0.57	
^{81}Rb	5.36± 0.08	286± 31
^{83}Rb	4.39± 0.09	
^{86}Y	5.41± 0.13	
^{87}Y	4.74± 0.07	1038± 66
^{89}Zr	4.90± 0.06	849± 58
^{89}Nb	6.70± 1.83	
^{90}Nb	4.22± 0.25	>530
^{90}Mo	5.78± 0.07	477± 113
$^{93}Mo^m$	5.23± 0.13	>338
^{93}Tc	5.54± 0.17	
^{94}Tc	5.29± 0.15	
^{94}Ru	5.25± 0.13	>77.1
^{95}Nb	2.79± 0.11	
$^{95}Tc^m$	3.80± 0.12	
^{95}Ru	4.87± 0.12	>56.1
^{96}Nb	5.92± 0.76	
^{96}Tc	3.68± 0.07	
^{97}Ru	3.82± 0.05	801± 28
^{97}Rh	4.44± 0.27	
^{99}Rh	3.21± 0.28	
$^{99}Rh^m$	4.38± 0.16	720± 44
^{99}Pd	3.48± 0.13	>33.2
^{100}Rh	3.09± 0.32	254± 54
^{100}Pd	3.01± 0.06	668± 101
$^{101}Rh^m$	2.46± 0.04	
^{101}Pd	2.91± 0.08	>159

^{102}Rh	2.63± 0.29	
^{102}Ag	2.44± 0.19	
^{103}Ag	1.91± 0.04	>73.1
^{104}Ag	1.25± 0.07	>7.29
^{105}Ag	0.90± 0.01	123± 16
^{105}Cd	1.68± 0.66	
^{106}Rh^{m}	3.48± 0.92	
^{106}Ag^{m}	0.52± 0.01	>18.0
^{107}In	3.76± 2.00	
^{108}In^{m}	2.02± 0.13	
^{109}In	2.15± 0.42	16.6± 3.4
^{112}Pd	3.64± 1.23	
^{112}Ag	3.52± 0.96	

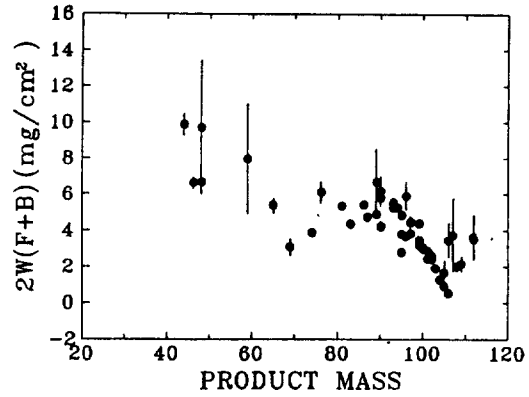

Figure 3. Dependence of the mean ranges 2W(F+B) on product mass number.

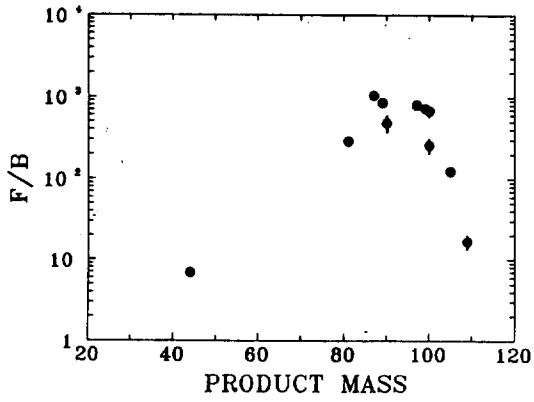

Figure 4. Dependence of forward-to-backward ratios F/B on product mass number.

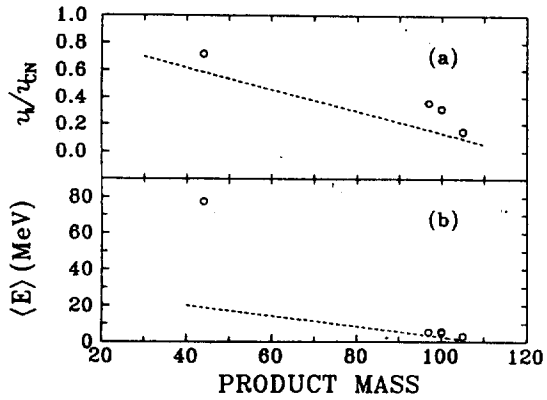

Figure 5. (a) Fractional momentum transfer $v_{\parallel}/v_{CN}$ shown as a function of product mass. Points, fit to data. The dashed line refers to a linear fit obtained in the interaction of silver with 86 MeV/nucleon ^{12}C ions. (b) The mean kinetic energies as a function of product mass. Points, fit to data. The dashed line refers to a linear fit obtained in the interaction of silver with 86 MeV/nucleon ^{12}C ions.

b. The fitted curve was extrapolated to A=119, thereby adding ~100 mb to R, in order to account for any missing trans-target products. It has been reported that light fragments at the energies of interest are formed in a binary process.[15] As a result, fragments with A<52 were excluded, because the yield of their partners with A>52 had been included in the integration procedure. The value of the total reaction cross section is in the vicinity of those obtained in the interactions of silver with ^{12}C ions.[6]

The results of the recoil measurements, expressed in terms of the average range, 2W(F+B), and the ratio of forward-to-backward emission, F/B, are listed in Table 3. The quantities F and B are the fractions of the total activity of a given nuclide found in the forward and backward catchers, respectively, and W is the target thickness in units of mg/cm^2. The tabulated uncertainties were determined in a similar way as those in the cross sections.

The average ranges and F/B ratios are plotted versus product mass number in Figure 3 and Figure 4, respectively. The ranges increase with decreasing product mass number, as observed in the interaction of silver with 86 MeV/nucleon ^{12}C.[3] Below A~70 this trend is broken, indicating a transition in reaction mechanism leading to these products. At this energy regime, the F/B ratios have been obtained only for some of the radionuclides. The values of F/B are found to be much larger than those obtained at the higher projectile energy.[3] For the transformation of the recoil data into kinematic quantities, the code written by Winsberg,[16] that is based on two-step vector mode, was used. The range-energy data was taken from Northcliffe and Schilling.[17] In a first step momentum is transferred to the target nucleus, resulting in an excited intermediate system moving with a velocity $v_{\parallel}$. The perpendicular velocity is assumed to be zero. In a second step, the intermediate system deexcites by particle emission giving the residual nucleus a velocity, V, in the moving frame. The distribution of kinetic energies, calculated from V, is assumed to have a Maxwellian form.

We have obtained kinematic quantities only for ^{44}Sc^{m}, ^{97}Ru, ^{100}Rh, ^{100}Pd and ^{105}Ag from the recoil data. The fractional momentum transfer, $v_{\parallel}/v_{CN}$, where v_{CN} is the velocity of the hypothetical compound nucleus, is plotted versus product mass in Figure 5a. The fractional momentum transfer is shown to be higher than that observed in the interaction of silver with 86 MeV/nucleon ^{12}C.[3] Owing to the lack of F/B-ratio data, the trend that the fractional momentum transfer increases with decreasing product mass could not be confirmed. However, the fractional momentum transfer for light products is found to be higher than that for heavy products. The values of $v_{\parallel}/v_{CN}$ in this energy regime are found

to be higher than those obtained at the higher energy. The mean kinetic energies are plotted versus product mass in Figure 5b, showing a similar behavior, as seen in the fractional momentum transfer.

Conclusion

The interaction of silver with 40 MeV/nucleon ^{14}N ions has been studied. The cross section is shown to increase with product mass. A striking feature is that nuclides with higher mass number than target mass are measured. This indicates that fusion mechanism could play a role at this energy.

The isobaric-yield distribution is near-Gaussian. The mass yield distribution peaks at A~96, decreases to a minimum at A~52, and increases at lower mass numbers. The isobaric-yield and mass yield distributions have been compared with the results of other intermediate-energy measurements. Both distributions are independent of projectile mass in this energy regime. The total reaction cross section was deduced by integration of the mass yield distribution to be 2.87± 0.43 b, which is in the vicinity of those obtained in the intermediate-energy ^{12}C-induced reactions.

The ranges increase with decreasing product mass, as observed in the interaction of silver with 86 MeV/nucleon ^{12}C ions. This trend is broken at A~70, indicating a transition in reaction mechanism leading to these products. Owing to the lack of the F/B-ratio data, the trend that the fractional momentum transfer and mean kinetic energy increase with decreasing product mass could not be confirmed. Both the fractional momentum transfer and mean kinetic energy for light products are found to be higher than those for heavy products. They are found to be higher than those at the higher energies, implying that there is a change in reaction mechanism.

Acknowledgment. We wish to thank Dr. R. Ronningen and the other members of the NSCL staff for their assistance and cooperation. This work was supported by Korea Science & Engineering Foundation and by the US Department of Energy.

References

1. Lund, T.; Molzahn, D.; Brandt, R.; Bergersen, B.; Eriksen, D.; Hagebo, E.; Haldorsen, I. R.; Bjornstad, T.; Richard-Serre, C. *Phys. Lett.* **1981**, *102B*, 239.
2. Lund, T.; Molzahn, D.; Bergersen, B.; Bjornstad, T.; Hagebo, E.; Haldorsen, I. R.; Richard-Serre, C.; The Isolde Collaboration *Z. Phys. A* **1982**, *306*, 43.
3. Lund, T.; Molzahn, D.; Bergersen, B.; Bjornstad, T.; Hagebo, E.; Haldorsen, I. R.; Richard-Serre, C.; The Isolde Collaboration *Phys. Lett.* **1982**, *116B*, 325.
4. Pouliot, J.; Chan, Y.; Dacal, A.; DiGregorio, D. E.; Harmon, B. A.; Knop, R.; Ortiz, M. E.; Plagnol, E.; Stokstad, R. G.; Moisan, C.; Potvin, L.; Rioux, C.; Roy, R. *Phys. Lett. B* **1989**, *223*, 16.
5. Badal , A.; Barbera, R.; Palmeri, A.; Pappalardo, G. S.; Riggi, F. *Phys. Rev. C* **1993**, *48*, 633.
6. Chung, Y. H.; Cho, S. Y.; Porile, N. T. *Nucl. Phys. A* **1991**, *533*, 170.
7. Cho, S. Y.; Chung, Y. H.; Porile, N. T.; Morrissey, D. J. *Phys. Rev. C* **1987**, *36*, 2349.
8. Cho, S. Y.; Porile, N. T.; Morrissey, D. J. *Phys. Rev. C* **1989**, *39*, 2227.
9. Hubert, F.; Fleury, A., Bimbot, R.; Gardes, D. *Ann. de Phys.* **1980**, *5*, 1.
10. Routti, J. T.; Prussin, S. G. *Nucl. Instr. Meth.* **1969**, *72*, 125.
11. Cumming, J. B. *National Academy of Sciences Report No. NAS-NS-3107*; U.S.A., 1962; p 25.
12. Reus, U.; Westmeier, W. *Atomic Data and Nucl. Data Tab.* **1983**, *29*, No. 1 & 2.
13. Porile, N. T.; Cole, G. D.; Rudy, R. C. *Phys. Rev. C* **1979**, *19*, 2288.
14. Rudstam, G. *Z. Naturforsch A* **1966**, *21*, 1027.
15. Charity, R. J.; McMahan, M. A.; Bowman, D. R.; Liu, Z. H.; McDonald, R. J.; Wozniak, G. J.; Moretto, L. G.; Bradley, S.; Kehoe, W. L.; Mignerey, A. C.; Namboodiri, M. N. *Phys. Rev. Lett.* **1986**, *56*, 1354.
16. Winsberg, L. W. *Nucl. Instr. Meth.* **1978**, *150*, 465.
17. Northcliff, L. C.; Schilling, R. F. *Nucl. Data Tables* **1970**, *A7*, 233.